

The Novel Hsp90 Inhibitor NXD30001 Induces Tumor Regression in a Genetically Engineered Mouse Model of Glioblastoma Multiforme

Haihao Zhu¹, Steve Woolfenden¹, Roderick T. Bronson³, Zahara M. Jaffer⁵, Sofia Barluenga⁷, Nicolas Winssinger⁷, Allan E. Rubenstein^{5,6}, Ruihong Chen⁵, and Al Charest^{1,2,4}

Abstract

Glioblastoma multiforme (GBM) has an abysmal prognosis. We now know that the epidermal growth factor receptor (EGFR) signaling pathway and the loss of function of the tumor suppressor genes *p16Ink4a/p19ARF* and *PTEN* play a crucial role in GBM pathogenesis: initiating the early stages of tumor development, sustaining tumor growth, promoting infiltration, and mediating resistance to therapy. We have recently shown that this genetic combination is sufficient to promote the development of GBM in adult mice. Therapeutic agents raised against single targets of the EGFR signaling pathway have proven rather inefficient in GBM therapy, showing the need for combinatorial therapeutic approaches. An effective strategy for concurrent disruption of multiple signaling pathways is via the inhibition of the molecular chaperone heat shock protein 90 (Hsp90). Hsp90 inhibition leads to the degradation of so-called client proteins, many of which are key effectors of GBM pathogenesis. NXD30001 is a novel second generation Hsp90 inhibitor that shows improved pharmacokinetic parameters. Here we show that NXD30001 is a potent inhibitor of GBM cell growth *in vitro* consistent with its capacity to inhibit several key targets and regulators of GBM biology. We also show the efficacy of NXD30001 *in vivo* in an EGFR-driven genetically engineered mouse model of GBM. Our findings establish that the Hsp90 inhibitor NXD30001 is a therapeutically multivalent molecule, whose actions strike GBM at the core of its drivers of tumorigenesis and represent a compelling rationale for its use in GBM treatment. *Mol Cancer Ther*; 9(9); 2618–26. ©2010 AACR.

Introduction

Glioblastoma multiforme (GBM) is the most common type of primary astrocytic tumor, as well as the most malignant. It is composed of poorly differentiated aggressive neoplastic cells that are characterized by explosive growth, invasiveness, and an innate resistance to current therapies (1). At present, the standard-of-care treatment for GBM consists of surgical resection when possible, followed by ionizing radiation with concomitant and adjuvant administration of the alkylating chemotherapeutic agent temozolomide. This vigorous regimen only

confers a median survival period of 14.6 months (2), reasserting the need for alternative measures.

Extensive molecular characterizations of GBMs have shown a number of genetic mutations and signaling abnormalities that are now recognized as drivers of uncontrollable growth, invasiveness, angiogenesis, and resistance to apoptosis (3, 4). GBMs are now categorized into proneural, neural, classical and mesenchymal subclasses according to recently characterized and specific gene expression-based molecular classifications (5, 6). In the classical subtype of GBMs, aberrant expression of epidermal growth factor receptor (EGFR) is observed in 100% of the cases (5). Deregulated, active EGFR results in overactivation of the Ras/Raf/mitogen-activated protein kinase and phosphoinositide 3-kinase/Akt signal transduction pathways, which are both recognized as major contributors to GBM growth and resistance to therapy. Reinforcing the Akt survival pathway in these GBMs is the observation that 95% of these tumors exhibit deletions or mutations within the tumor suppressor gene *PTEN* and 100% are homozygously deleted or mutated in the *INK4a/ARF (CDKN2a)* locus (5). This triple combination of activated EGFR, loss of *CDKN2a*, and *PTEN* loci is found in over a quarter of all GBM patients (5).

Loss of the *INK4a/ARF (CDKN2a)* locus corresponds to a key event in tumorigenesis. Allosteric binding of the

Authors' Affiliations: ¹Molecular Oncology Research Institute and ²Department of Neurosurgery, Tufts Medical Center, ³Department of Pathology, Harvard Medical School, and ⁴Tufts University School of Medicine, Tufts University, Boston, Massachusetts; ⁵NexGenix Pharmaceuticals, and ⁶Department of Neurology, New York University Langone Medical Center, New York, New York; and ⁷Institut de Science et Ingénierie Supramoléculaires, Université de Strasbourg, Strasbourg, France

Corresponding Authors: Al Charest, Molecular Oncology Research Institute, Tufts Medical Center, 800 Washington Street Box 5609, Boston, MA 02111. E-mail: alain.charest@tufts.edu or Ruihong Chen, NexGenix Pharmaceuticals, 152 West 57th Street, New York, NY 10019. Phone: 617-636-8876; Fax: 627-636-5277. E-mail: rchen@nexgenixpharm.com

doi: 10.1158/1535-7163.MCT-10-0248

©2010 American Association for Cancer Research.

INK4 class of cell-cycle inhibitors to the cyclin-dependent kinases CDK4/6 abrogates their binding to D-type cyclins, a prerequisite for CDK4/6-mediated phosphorylation of retinoblastoma (Rb) family members and progression through the cell cycle. The tumor suppression activities of the INK4 class of proteins lies in the concept that deletion of p16INK4a in tumors facilitates the formation of CDK4/6-CyclinD complexes, shifts Rb-family proteins in a hyperphosphorylated state, and thus promotes unregulated cell-cycle progression (reviewed in ref. 7). In this context, inhibitors of CDK4/6 or CyclinD activities would counteract the effects of loss of INK4 class of proteins in tumor cells and represent an effective strategy against cancer (8).

Heat shock protein 90 (Hsp90) is a molecular chaperone that maintains the conformation and activity of specific substrates (client proteins), including key proteins involved in signal transduction, cell cycle control, and regulation of transcription. Many Hsp90 client proteins are responsible for initiation and maintenance of GBMs including EGFR, Akt, CDK4, and CyclinD1. Compounds that block Hsp90 ATPase activity have been shown to induce proteasomal degradation of cancer-related Hsp90 client proteins (recently reviewed in ref. 9) and are currently being assessed in clinical trials for cancer treatment (10). The ability of Hsp90 inhibitors to simultaneously target multiple signal transduction pathways involved in the proliferation and survival of GBMs makes these compounds ideal therapeutic candidates for the treatment of GBMs and other cancers characterized by multifaceted etiologies.

In this article, we show that the novel small molecule second-generation Hsp90 inhibitor NXD30001 (pochoximeA; refs. 11–13) has potent pharmaceutical and pharmacologic properties in a genetically engineered preclinical mouse model of GBM (14) where its mechanisms of action relate to an effective Hsp90 inhibition. These results provide a preclinical rationale to support escalation to clinical trials with NXD30001 in patients with GBM.

Materials and Methods

Transgenic animals and tumor induction procedures

All mouse procedures were done in accordance with Tufts University's recommendations for the care and use of animals and were maintained and handled under protocols approved by the Institutional Animal Care and Use Committee. Intracranial glioblastoma tumors were induced as follows. Adult compound *Col1a1^{tm2(CAG-EGFR*)Char/tm2(CAG-EGFR*)Char}; Cdkn2a^{tm1Rdp/tm1Rdp}; Pten^{tm1Hwu/tm1Hwu}; Tg(CAG-luc)C6Char* conditional transgenic animals (14, 15) of 3 months of age or above were anesthetized with an i.p. injection of ketamine/xylazine (ketamine 100–125 mg/kg, xylazine 10–12.5 mg/kg), mounted on a stereotaxic frame and processed for injections as described before (14), using a pulled glass pipet mounted onto a Nanoject II injector (Drummond Scientific

Company) to inject 250 nL aliquot of an adeno-CMV-Cre virus (GTVc, U Iowa) over a period of 10 minutes. Following retraction of the pipet, the burr hole was filled with sterile bone wax, the skin was drawn up and sutured, and the animal was placed in a cage with a padded bottom atop a surgical heat pad until ambulatory.

Cell culture

All mouse and human GBM primary cell cultures derived from tumors were maintained in DMEM supplemented with 10% (v/v) fetal bovine serum as described (14, 16). Primary cultures of mouse astrocytes were established according to published protocols (17). 17-allylamino-17-demethoxygeldanamycin (17-AAG) was obtained from Sigma.

Immunoblot analysis

Western blots were done as follows. Total cell lysates were harvested using radioimmunoprecipitation assay buffer supplemented with 5 mmol/L Na₃VO₄ and protease inhibitor cocktail. Concentrations of lysates were determined using protein quantification reagents (Bio-Rad). Lysates (40 µg) were separated by SDS-PAGE and electrotransferred to polyvinylidene difluoride membrane (Immobilon P, Millipore). Blots were blocked in TBS 0.1% (v/v) Tween-20 (TBS-T), 1% (wt/v) bovine serum albumin (BSA), and 5% (wt/v) nonfat dry milk (Bio-Rad) for 1 hour on a shaker. Primary antibodies were added to blocking solution and incubated overnight at 4°C on a shaker. Blots were washed several times with TBS-T-BSA, and secondary antibodies were added at 1:10,000 dilutions into TBS-T BSA and incubated for 1 hour at room temperature on a shaker. After several washes, enhanced chemiluminescence (ECL) reactions were done as described by the manufacturer (Western Lightning Kit, Perkin Elmer). The antibodies and respective dilutions used in these studies were anti-EGFR (Cell Signaling Technology; 1:2,000), anti-total AKT (Cell Signaling Technology; 1:5,000), anti-dynamin (BD Transduction Laboratories; 1:2,000), anti-CDK4 (Santa Cruz Biotechnology; 1:5,000), anti-cyclin D1 (Santa Cruz Biotechnology; 1:250), and cleaved-caspase 3 (Cell Signaling Technology; 1:1,000).

Cell proliferation and apoptosis analysis

GBM cells were seeded at a density of 5,000/well on 96-well plates, cultured in the presence of drugs or vehicle for 36 hours, and subjected to a 2,3-bis[2-methoxy-4-nitro-S-sulfophenyl]H-tetrazolium-5-carboxanilide inner salt cell proliferation assay (Roche) in quadruplicate according to the manufacturer's specifications. For detection of apoptosis, cells were plated in 8-well Chamber slides (BD Biosciences) at a density of 10,000 cells/well and treated with NXD30001 for the indicated time, fixed with fresh 4% paraformaldehyde for 15 minutes and stained with Hoechst 33258 dye (5 µg/mL for 5 minutes) and scored for apoptosis. Apoptotic cells were visualized by fluorescence microscopy and reported as percent apoptotic

pyknotic nuclei over total nuclei as averages of three independent areas.

Histology

Deeply anesthetized animals were transcardially perfused with cold PBS followed by freshly made 4% paraformaldehyde. Brains were excised, rinsed in PBS, and postfixed in 4% paraformaldehyde at 4°C for 30 minutes. Serial 2-mm coronal sections were cut using a brain mold. Fixed tissues were embedded in paraffin, sectioned at 5 to 10 $\mu\text{mol/L}$, and stained with H&E (Sigma) for histopathologic analysis.

Pharmacokinetic studies

Pharmacokinetic experiments were conducted in mice to evaluate the exposure of NXD30001 in plasma and brain tissues following a single dose or a repeat dose schedule (every other day for a total of 7 doses) of i.v. administration. The study was done at BioDuro (headquarters in San Diego, CA). CD-1 mice (8 weeks of age, male, 29–36 g body weight) were used for the study. NXD30001 was reconstituted in the vehicle (6% *N,N*-Dimethylacetamide, 10% soybean oil, 5% Tween 80, and 79% water) at 7 mg/mL for the single-dose regimen and 2.5 mg/mL for the repeat-dose schedule. Three mice per time point were dosed at 70 mg/kg and dosing volume of the drug solutions was adjusted with vehicle such that the dosage for each mouse was corrected for fasted body weight. The concentration of dosing solution was confirmed by liquid chromatography/tandem mass spectrometry (LC/MS-MS). Blood samples via cardiac puncture and brain tissues were collected at 0.5, 1, 2, 4, 8, 12, 24, and 48 hours following administration of the compound. The blood samples were temporarily put on ice and then centrifuged at 10,000 rpm for 3 to 5 minutes to separate for plasma. Plasma samples were stored at -20°C until bioanalysis. The brain samples were washed quickly with saline at 4°C and homogenized. The compounds in the plasma and brain homogenates were extracted with 10 volumes of methyl tertiary butyl ether, and supernatants were dried under N_2 . The concentrations of the test compounds in plasma and brain were determined using a LC/MS-MS method. An Agilent Zorbax C18 column (2.1 \times 50 mm, 3.5 μm) was used at a temperature of 25°C. The mobile phase A was water (0.1% formic acid) and the mobile phase B was methanol (0.1% formic acid). The flow rate was 400 $\mu\text{L}/\text{minute}$ and the injection volume was 10 μL . The lower limit of quantification (LLOQ) of the bioanalytical method was 1 ng/mL for plasma and 0.5 ng/mL for brain. The range was 1 to 2,000 ng/mL for plasma and 0.5 to 500 ng/mL for brain. All solvents and chemicals were of analytical grade or better. Pharmacokinetic parameters were calculated using WinNonlin (V5.2.) and noncompartment model. Concentrations of NXD30001 and 17-AAG were measured in brain tissues of BT474 xenograft-bearing NCR-Nude mice after single i.p. injections at the indicated concentrations after 6, 12, 24, and 48 hours (13).

Concentrations of drugs from brain homogenates were determined by LC/MS-MS. A Shimadzu VP System (column: 2 \times 10 mm Peek Scientific Duragel G C18 guard cartridge) was used. The mobile phase A was water (0.2% formic acid) and the mobile phase B was methanol (0.2% formic acid). The flow rate was 400 $\mu\text{L}/\text{minute}$ and the injection volume was 100 μL . The gradient was 5% B for 0.5 minutes and then 5% to 95% B in 2 minutes. Applied Biosystems/MDS SCIEX API 3000 was used. The LLOQ of the bioanalytical method was 4.6 ng/mL for both NXD30001 and 17-AAG.

Tumor growth monitoring by bioimaging and NXD30001 treatment of mice

Growth of GBM tumors was monitored noninvasively through bioluminescence as described previously (15), using the IVIS 200 imaging system (Xenogen). Live imaging of animals was done as follows. Areas of focus for imaging were depilated using commercial depilatory creams. All of the images were taken 10 minutes after i.p. injection of luciferin (225 mg/kg; Xenogen) to allow proper distribution of luciferin, with a 60-second photon acquisition during which mice were sedated via continuous inhalation of 3% isoflurane. Signal intensity was quantified for defined regions of interest as photon count rate per unit body area per unit solid angle subtended by the detector (units of photons/s/cm²/steradian). All image analyses and bioluminescent quantification were done using Living Image software v. 2.50 (Xenogen). NXD30001 was dissolved in vehicle (10% v/v *N,N*-Dimethylacetamide, 5% v/v Tween 20, 15% v/v cremophor, 70% v/v saline). Mice bearing tumors that reached 10⁶ relative light units were dosed by i.p. injections with 100 mg/kg three times weekly for two weeks followed by twice weekly for the times indicated.

IC₅₀ and statistical analysis

IC₅₀ values and curve fitting were done using Prism 5.0 (GraphPad Software) with nonlinear regression analysis. Statistical analyses were carried out using two-tailed, unpaired Student's *t* test. Comparison of overall survival rates was done using log-rank analysis, and Kaplan-Meier curves were generated using Prism 5.0. *P* values were calculated using a Mantel-Cox two-tailed test for significance.

Results

NXD30001 accumulates in brain tissue

A major impediment to robust drug efficacy against GBM is the inability of therapeutic compounds to access tumor cells that have migrated into healthy parenchyma and that are thus protected by an intact blood brain barrier (BBB). Pharmacokinetic studies of NXD30001 in mice indicate that i.v. administered NXD30001 disperses with favorable kinetics and accumulates well within brain tissues (Table 1A). We further assessed the ability of NXD30001 to penetrate the BBB and its central

Table 1. Pharmacokinetic study of NXD30001 in mice**(A) Pharmacokinetic profile**

	AUC _(0-t)	C _{max} (ng/g)	C ₀ (ng/mL)	T _{max} (h)	T _{1/2} (h)	CL (mL/min/kg)	V _d (L/kg)	Ratio of AUC _(0-t) (brain/plasma)
Single dose								
Plasma (ng.h/mL)	5,346	NA	2,140	NA	2.74	217	51.5	NA
Brain (ng.h/g)	1,073	223	NA	0.5	4.07	NA	NA	0.201
Repeated doses								
Plasma (ng.h/mL)	6,960	NA	4,530*	NA	5.4	59.8	27.9	NA
Brain (ng.h/g)	940	210	NA	0.25	8.99	NA	NA	0.135

(B) Brain concentrations

Time (h)	NXD30001 (ng/g)		17-AAG (ng/g)
	100 mg/kg	150 mg/kg	75 mg/kg
6	675.5	1439.5	2.6
12	823	3424	ND
24	271	899.5	ND
48	10.7	115.5	ND

NOTE: Concentrations of NXD30001 in plasma and brain homogenates were determined by LC/MS-MS after a single i.v. injection at 70 mg/kg or after repeated i.v. injections at 25 mg/kg every other day for a total of 7 doses (A). Brain concentrations of HSP90 inhibitors in mice (B). Concentrations of NXD30001 and 17-AAG in brain homogenates were determined by LC/MS-MS after a single i.p. injection.

Abbreviations: AUC_{0-t}, area under the curve from the time of dosing to the time of the last observation; C_{max}, maximum concentration; C₀, concentration at time 0; T_{max}, time of the maximum concentration; T_{1/2}, terminal half-life; CL, clearance; V_d, volume of distribution at terminal phase; NA, not applicable; ND, not detected.

* The concentration shown is the average concentration at 0.5 hour rather than C₀.

nervous system (CNS) retention by measuring its concentration in brain tissues following i.p. injections (Table 1B). NXD30001 reached a maximal concentration of 823 ng/g after a single dose of 100 mg/kg after 12 hours. Conversely, the accumulation of 17-AAG in mouse brain rapidly declined to undetectable levels 6 hours after a single i.p. dose. In addition, a multiple-dose pharmacokinetic experiment (seven every other day i.v. dosing at 25mg/kg) was conducted to determine if there is drug accumulation with repeat dosing (Table 1A). Despite the lower dose used in the repeat-dose experiment, plasma and brain concentrations after multiple doses were greater than or similar to those after a single i.v. dose at 70 mg/kg. Similarly, plasma and brain area under the curve (AUC) values were comparable for both single- and repeat-dose experiments. The ratios of brain/plasma AUC were not significantly different. These results suggest some accumulation of NXD30001 after the repeat dose although very little NXD30001 was detected in plasma or brain prior to the last dose (<10 ng/mL or 10 ng/g).

NXD30001 is a potent inhibitor of GBM cell proliferation *in vitro*

Having shown that NXD30001 has promising pharmacokinetic parameters *in vivo*, we treated EGFR-driven

mouse GBM tumor primary cell cultures (14) and primary astrocytes cultures with NXD30001. Treatment of these cells with NXD30001 led to a dose- and time-dependent inhibition of GBM cell growth but not of astrocytes (Fig. 1A and B). The growth inhibition that is observed in Fig. 1A and B was concurrent with the degradation of the Hsp90 client proteins EGFR, Akt, Cdk4, and CyclinD1 (Fig. 1C). It has been previously shown that Hsp90 inhibition in gliomas can result in apoptosis (18). Similarly, the growth inhibition observed correlated with a 10-fold increase in apoptosis level in these cells as measured by the production of pyknotic nucleated cells and the appearance of cleaved-caspase 3 (Fig. 2). Taken together, these data show that NXD30001 prevents GBM cell growth by promoting apoptosis and degradation of Hsp90 client proteins. We then expanded these studies using a panel of primary GBM tumor lines established from mouse tumors as described (14). In these cells, NXD30001 inhibited cell proliferation with nanomolar IC₅₀ potency and was reliably more potent than 17-AAG (Table 2). To correlate these results to human GBMs, we tested NXD30001 on a panel of human GBM primary cultured cells. Treatment of these cells with NXD30001 also showed nanomolar potency and enhanced efficacy over 17-AAG (Table 2). When compared directly against 17-AAG, NXD30001 was between

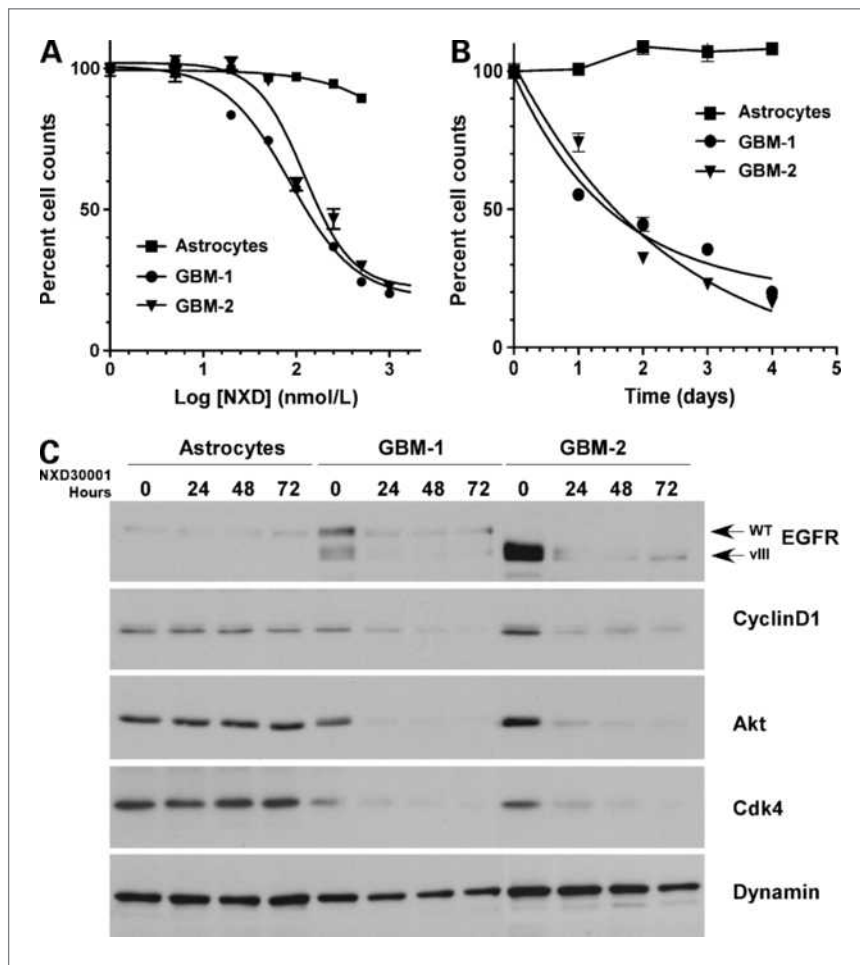


Figure 1. Efficacy of NXD30001 on GBM cells. A, mouse primary cultures of astrocytes and GBM cell cultures (GBM-1 and -2) were grown in the presence of increasing concentrations of NXD30001 for 24 hours, counted, and cell numbers were plotted as percent of untreated cells. B, cells were treated with 250 nmol/L of NXD30001 for the indicated amount of time, and viable cells were counted and plotted as percent of untreated cells. C, Western blot showing the depletion of the indicated Hsp90 client proteins (and dynamin as a control) in GBM-1 and -2 cultures and primary mouse astrocytes treated with 250 nmol/L of NXD30001 for the indicated times. GBM-1 cells coexpress wild-type (WT) and vIII EGFR, and GBM-2 cells express EGFR vIII. Data points, mean values of triplicates; error bars, SD.

0.4- and 9.8-fold more active at inhibiting GBM tumor cell growth. The cellular response to Hsp90 inhibition by NXD30001 was assessed by comparing the expression levels of the Hsp90 client proteins EGFR, Akt, CyclinD1,

and CDK4 by immunoblot analysis before and after NXD30001 treatment (Fig. 3). In all cultures tested, treatment of GBM cells with NXD30001 led to a significant reduction in the levels of these client proteins.

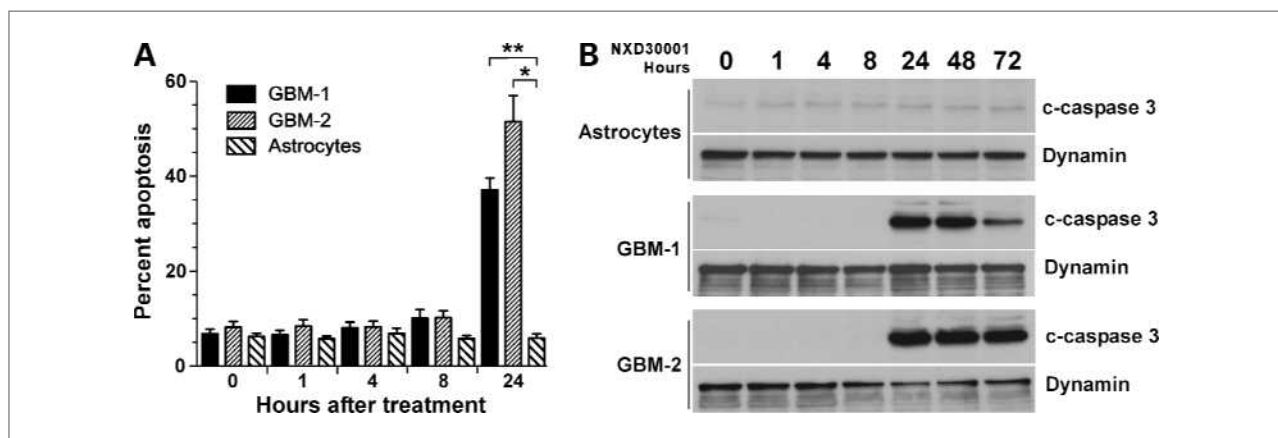


Figure 2. NXD30001 treatment of GBM cells leads to apoptosis. A, cells were exposed to 250 nmol/L of NXD30001 for the indicated times, fixed, and stained, and levels of apoptosis were reported as percentage of pyknotic cells relative to total number of cells. B, cells were treated with 250 nmol/L of NXD30001 for the indicated times, and lysates were processed for Western blot analysis to detect the levels of cleaved-caspase 3. Error bar, SD. * and **, $P < 0.0001$ *t*-test.

Table 2. Cytotoxicity of NXD30001 and 17-AAG in mouse and human GBM cultures as determined by cell proliferation assays

GBM cultures	NXD30001 IC ₅₀ (nmol/L)	17-AAG IC ₅₀ (nmol/L)
Mouse		
2414	31.7 ± 4.9	205.1 ± 13.1
46	54.3 ± 12.5	91.9 ± 1.4
69	73.4 ± 2.5	91 ± 4.3
42	73.8 ± 0.7	165.5 ± 24.9
2736	77.6 ± 2.8	381 ± 24.1
GBM-1	78.3 ± 8.3	207.5 ± 9.6
41	80.2 ± 5.9	100.2 ± 5.0
GBM-2	110.8 ± 9.4	1,096.4 ± 118.6
2000	115.4 ± 9.4	344.8 ± 75.5
2227	134.3 ± 7.7	712 ± 54.4
2231	146.1 ± 3.7	737.3 ± 72.0
2415	251.1 ± 57.7	328.8 ± 50.1
102	360.5 ± 21.6	626.2 ± 6.0
103	575.6 ± 14.8	793.5 ± 28.7
Human		
GBM15	60.7 ± 0.5	110.4 ± 13.4
GBM43	86.3 ± 0.2	86.9 ± 2.3
GBM39	111.6 ± 1.0	241.7 ± 1.2
GBM59	232 ± 13.2	211.2 ± 11.0
GBM6	1,217.5 ± 35.1	531.7 ± 5.0
GBM12	2,334 ± 60.0	2,575.9 ± 166.5
GBM22	5,261.6 ± 152.2	4,668.2 ± 148.0
GBM8	5,691.3 ± 449.6	8,010.8 ± 542.6

NOTE: Results are presented as the mean ± SD of three independent experiments.

NXD30001 treatment increases survival and induces GBM tumor regression in mice

In light of these results, we evaluated the efficacy of NXD30001 in mice bearing GBM tumors. First, we crossed our EGFR-based model to a conditional luciferase reporter strain that we had recently characterized (15) and in which we showed a robust relationship between bioluminescent light emission and GBM tumor volume. Tumor growth is therefore monitored longitudinally, and increases in bioluminescence imaging (BLI) output linearly correspond to GBM volume. More importantly, this approach allows for consistency in initiation of treatment. The rationale behind the utilization of this strain as a reporter of tumor size is that only cells that are exposed to Cre recombinase, and therefore giving rise to EGFR-dependent GBMs, express the bioluminescent marker luciferase. This approach provides a high signal-to-noise ratio, which is a foremost requirement for quantitative bioimaging.

Cohorts of animals were established and developing brain tumors were monitored periodically by BLI to

assess relative tumor volumes and growth rates. Animals reaching a bioluminescent signal output of $>8 \times 10^6$ p/s/cm²/sr were randomized to treatment with either vehicle or 100 mg/kg of NXD30001 i.p. three times weekly ($\times 2$) then twice weekly for the remaining course of treatment. Once treatment was initiated, BLI monitoring was suspended because luciferase is a client protein of Hsp90 (19), potentially inducing compromising readout accuracy. Mice were treated for over 100 days or until moribund, and the surviving mice were reimaged periodically posttreatment discontinuation until termination of study (Fig. 4A). Cohorts of treated and vehicle control untreated mice were monitored, and Kaplan-Meier survival curves were established (Fig. 4B). All of the vehicle control-treated mice succumbed to GBM within ~ 30 days post-Ad-Cre injection whereas half of the treated animals survived longer than 180 days (Fig. 4B), at which point they were processed for histopathologic analysis. Treatment of brain tumor-bearing mice with NXD30001 resulted in a statistically significant prolongation in survival. For these surviving animals, histologic analysis of H&E-stained paraffin-embedded brain sections revealed the presence of few remaining tumor cell clusters (Fig. 4C, arrows). It has been reported that exposure to 17-AAG, which is currently in clinical evaluation for various cancers (10), results in dose-limiting hepatotoxicity. In contrast, both short- and long-term NXD30001 exposure in mice does not result in hepatotoxicity (data not shown and ref. 13).

Discussion

The deadly nature of GBM lies in its inherent ability to migrate and infiltrate within the nondiseased brain. Recurrence is the norm and typically occurs within a few centimeters from the tumor margins, an area physiologically and physically protected from the effects of therapeutic agents by the BBB. As such, the ineffectiveness of systemically administered chemotherapeutic drugs in treating gliomas has long been attributed to the impermeability of the BBB (20, 21). Therefore, successful agents against GBM will require a heightened penetration of the BBB and superior CNS retention kinetics. The recent inclusion of the lipophilic compound temozolomide as a major component of first line treatment for GBM underscores these principles (22, 23).

Recent advances in the molecular characterization of GBMs indicate that single target agent monotherapies are less likely to produce significant impact on the treatment front (24). It is also becoming clear that successful treatments against GBM will arise from multitarget approaches. Single agents capable of striking multiple targets at once will offer a tremendous advantage over combinatorial drug cocktails given the often synergistic multidrug toxicities.

Inhibition of Hsp90 activity results in the degradation of several proteins that play key roles in tumorigenesis. 17-AAG is a well-known Hsp90 inhibitor that is currently

the farthest advanced in clinical evaluation for solid tumors (10). Given that efficient penetration through the BBB and prolonged CNS retention are absolutely necessary for the successful treatment of gliomas, our findings that NXD30001 has superior brain pharmacokinetics to 17-AAG has significant clinical implications and underscores the applicability of NXD30001 for GBM treatment.

Our *in vitro* studies showed a potent inhibition of GBM growth by NXD30001. This successful inhibition of cell growth and induction of cell death can be explained by the relative biological credence GBM cells impart on Hsp90 client protein targets for survival. For example, the EGFR-phosphoinositide 3-kinase-Akt axis, which is reinforced by loss of *PTEN*, is a key driver of GBM survival through a variety of mechanisms (reviewed in ref. 25). Elimination of expression of both EGFR and Akt, considered a nodal point in this pathway, in GBMs robs these cells from potent prosurvival signals. In addition, loss of Ink4a in these tumors shifts the CDK4/CyclinD equilibrium towards duplex formation and deregulated cell cycle progression. Similarly, inhibition of Hsp90 leads to considerable decreases in the levels

of both CDK4 and CyclinD1, thus counteracting the effects of the functional loss of Ink4a in tumor cells.

These observations were correlated *in vivo* by a prolonged statistically significant survival of GBM-bearing mice when treated with NXD30001. The presence of these cells in the long-term surviving mice suggest that a protracted and sustained regimen in treating patients with NXD30001 may be required for complete tumor eradication or to maintain the remaining cells in a nonproliferative state. Given the absence of toxicity observed in the treated animals, extended treatment is realistic.

Strong biological rationales have driven the use of Hsp90 inhibitors for the treatment of solid tumors, some of which are in various phases of clinical trials (10). Our data show that NXD30001 treatment of EGFR, Ink4a/Arf-PTEN-null driven *de novo* GBM tumors in a genetically engineered mouse model is an effective therapeutic strategy. Given the promising pharmacokinetic profile of NXD30001, persistent treatment for GBM patients is therefore a realistic option. The preclinical work that is described herein suggests that NXD30001 may prove to have therapeutic efficacy in GBM patients and should be further pursued clinically.

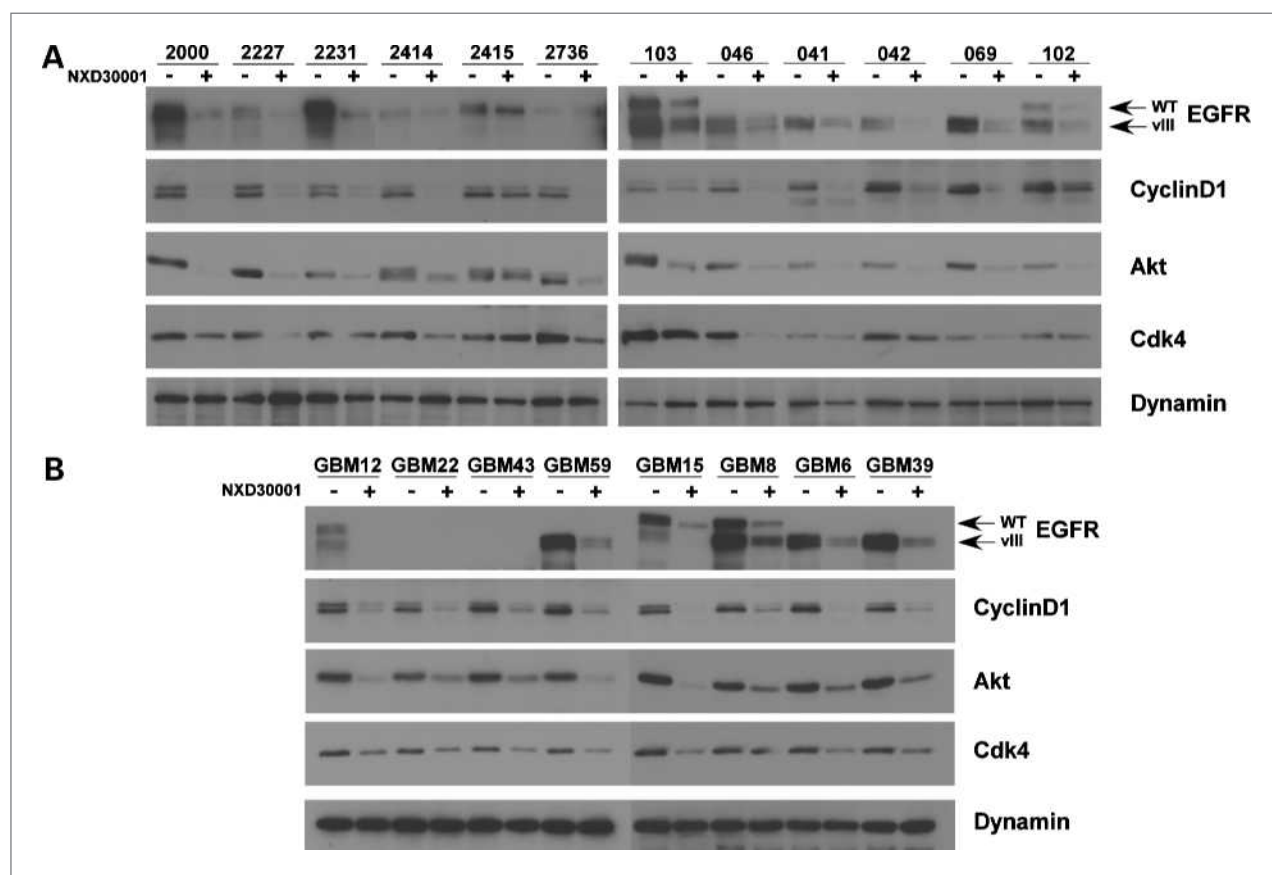


Figure 3. NXD30001 depletes Hsp90 client proteins in GBM cells. NXD30001 treatment of mouse (A) and human (B) primary GBM culture cells depletes the Hsp90 client proteins EGFR, Akt, Cdk4, and CyclinD1. Cells were treated with 250 nmol/L of NXD30001 or vehicle for 24 hours before preparing lysates. Equivalent amount of lysates were subjected to Western blot using antibodies against the indicated proteins.

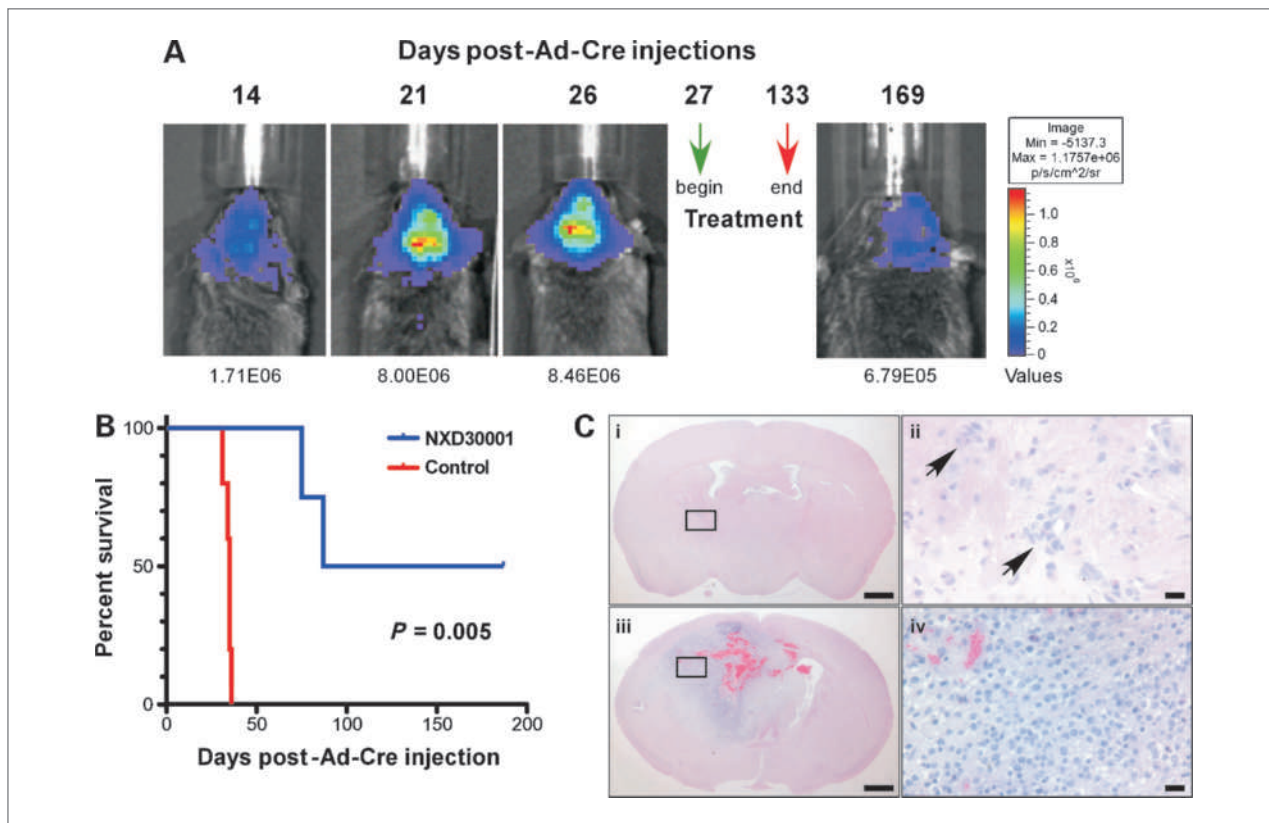


Figure 4. NXD30001 treatment of GBM tumor mice. **A**, study paradigm. Example of BLI outputs for a given mouse imaged 14, 21, and 26 days post tumor induction to determine the time of treatment initiation ($>8 \times 10^6$ p/s/cm²/sr; green arrow). Mice were dosed three times weekly ($\times 2$ weeks) and then twice weekly at 100 mg/kg in vehicle for >100 days. Control mice were given vehicle only. Animals were reimaged periodically over a period of time posttreatment (a 36 day postcessation of Rx is shown). **B**, Kaplan-Meier survival curves of EGFRvIII-driven GBM-bearing mice treated with NXD30001 or placebo according to the paradigm in **A**. Control, $n = 5$; treated, $n = 4$. **C**, photomicrographs of H&E-stained paraffin-embedded coronal brain sections (at the level of Ad-Cre injections) of treated (i and ii) and control vehicle-treated (iii and iv) mice (ii and iv are high-magnification photomicrographs of the insets in i and iii, respectively). Scale bars, i and iii, 1 mm; ii and iv, 25 μ m.

Disclosure of Potential Conflicts of Interest

R. Chen, A.E. Rubenstein, and Z.M. Jaffer are all employees of Nexgen Pharmaceuticals Holdings Ltd., a privately held, for-profit entity that owns the rights to NXD30001 and its analog compounds and is pursuing a development program for these compounds for glioblastoma and other indications.

Acknowledgments

We thank Drs. Kenneth Hung and Jaime Acquaviva for critical review of the manuscript.

Grant Support

A. Charest was supported by NIH grants U01CA141556-0109, ACS Research Scholar Grant 117409, Tufts Medical Center Research Award and The Neely Foundation for Cancer Care and Research. R. Chen was partially supported by NIH SBIR grant 1R43NS066546-01.

The costs of publication of this article were defrayed in part by the payment of page charges. This article must therefore be hereby marked *advertisement* in accordance with 18 U.S.C. Section 1734 solely to indicate this fact.

Received 03/11/2010; revised 05/26/2010; accepted 06/28/2010; published OnlineFirst 07/19/2010.

References

- Kleihues P, Cavenee WK. Pathology and genetics of tumours of the nervous system. Lyon: IARC Press; 2000.
- Stupp R, Mason WP, van den Bent MJ, et al. Radiotherapy plus concomitant and adjuvant temozolomide for glioblastoma. *N Engl J Med* 2005;352:987–96.
- Parsons DW, Jones S, Zhang X, et al. An integrated genomic analysis of human glioblastoma multiforme. *Science* 2008;321:1807–12.
- McLendon R, Friedman A, Bigner D, et al. Comprehensive genomic characterization defines human glioblastoma genes and core pathways. *Nature* 2008;455:1061–8.
- Verhaak RG, Hoadley KA, Purdom E, et al. Integrated genomic analysis identifies clinically relevant subtypes of glioblastoma characterized by abnormalities in PDGFRA, IDH1, EGFR, and NF1. *Cancer Cell* 2010;17:98–110.
- Phillips HS, Kharbanda S, Chen R, et al. Molecular subclasses of high-grade glioma predict prognosis, delineate a pattern of disease progression, and resemble stages in neurogenesis. *Cancer Cell* 2006;9:157–73.
- Kim WY, Sharpless NE. The regulation of INK4/ARF in cancer and aging. *Cell* 2006;127:265–75.

8. Hirai H, Kawanishi N, Iwasawa Y. Recent advances in the development of selective small molecule inhibitors for cyclin-dependent kinases. *Curr Top Med Chem* 2005;5:167–79.
9. Matts RL, Manjarrez JR. Assays for identification of Hsp90 inhibitors and biochemical methods for discriminating their mechanism of action. *Curr Top Med Chem* 2009;9:1462–78.
10. Kim YS, Alarcon SV, Lee S, et al. Update on Hsp90 Inhibitors in clinical trial. *Curr Top Med Chem* 2009;9:1479–92.
11. Barluenga S, Fontaine JG, Wang C, et al. Inhibition of HSP90 with pochoximes: SAR and structure-based insights. *Chembiochem* 2009;10:2753–9.
12. Barluenga S, Wang C, Fontaine JG, et al. Divergent synthesis of a pochonin library targeting HSP90 and in vivo efficacy of an identified inhibitor. *Angew Chem Int Ed Engl* 2008;47:4432–5.
13. Wang C, Barluenga S, Koripelly GK, et al. Synthesis of pochoxime prodrugs as potent HSP90 inhibitors. *Bioorg Med Chem Lett* 2009;19:3836–40.
14. Zhu H, Acquaviva J, Ramachandran P, et al. Oncogenic EGFR signaling cooperates with loss of tumor suppressor gene functions in gliomagenesis. *Proc Natl Acad Sci U S A* 2009;106:2712–6.
15. Woolfenden S, Zhu H, Charest A. A Cre/LoxP conditional luciferase reporter transgenic mouse for bioluminescence monitoring of tumorigenesis. *Genesis* 2009;47:659–66.
16. Sarkaria JN, Carlson BL, Schroeder MA, et al. Use of an orthotopic xenograft model for assessing the effect of epidermal growth factor receptor amplification on glioblastoma radiation response. *Clin Cancer Res* 2006;12:2264–71.
17. Weinstein DE. Isolation and purification of primary rodent astrocytes. *Curr Protoc Neurosci* 2001. Chapter 3:Unit 3 5.
18. Nomura M, Nomura N, Newcomb EW, Lukyanov Y, Tamasdan C, Zagzag D. Geldanamycin induces mitotic catastrophe and subsequent apoptosis in human glioma cells. *J Cell Physiol* 2004;201:374–84.
19. Galam L, Hadden MK, Ma Z, et al. High-throughput assay for the identification of Hsp90 inhibitors based on Hsp90-dependent refolding of firefly luciferase. *Bioorg Med Chem* 2007;15:1939–46.
20. Muldoon LL, Soussain C, Jahnke K, et al. Chemotherapy delivery issues in central nervous system malignancy: a reality check. *J Clin Oncol* 2007;25:2295–305.
21. Nies AT. The role of membrane transporters in drug delivery to brain tumors. *Cancer Lett* 2007;254:11–29.
22. Stupp R, van den Bent MJ, Hegi ME. Optimal role of temozolomide in the treatment of malignant gliomas. *Curr Neurol Neurosci Rep* 2005;5:198–206.
23. Hegi ME, Diserens AC, Gorlia T, et al. MGMT gene silencing and benefit from temozolomide in glioblastoma. *N Engl J Med* 2005;352:997–1003.
24. Stommel JM, Kimmelman AC, Ying H, et al. Coactivation of receptor tyrosine kinases affects the response of tumor cells to targeted therapies. *Science* 2007;318:287–90.
25. Engelman JA. Targeting PI3K signalling in cancer: opportunities, challenges and limitations. *Nat Rev Cancer* 2009;9:550–62.

Molecular Cancer Therapeutics

The Novel Hsp90 Inhibitor NXD30001 Induces Tumor Regression in a Genetically Engineered Mouse Model of Glioblastoma Multiforme

Haihao Zhu, Steve Woolfenden, Roderick T. Bronson, et al.

Mol Cancer Ther 2010;9:2618-2626. Published OnlineFirst July 19, 2010.

Updated version Access the most recent version of this article at:
doi:[10.1158/1535-7163.MCT-10-0248](https://doi.org/10.1158/1535-7163.MCT-10-0248)

Cited articles This article cites 23 articles, 5 of which you can access for free at:
<http://mct.aacrjournals.org/content/9/9/2618.full#ref-list-1>

Citing articles This article has been cited by 2 HighWire-hosted articles. Access the articles at:
<http://mct.aacrjournals.org/content/9/9/2618.full#related-urls>

E-mail alerts [Sign up to receive free email-alerts](#) related to this article or journal.

Reprints and Subscriptions To order reprints of this article or to subscribe to the journal, contact the AACR Publications Department at pubs@aacr.org.

Permissions To request permission to re-use all or part of this article, use this link
<http://mct.aacrjournals.org/content/9/9/2618>.
Click on "Request Permissions" which will take you to the Copyright Clearance Center's (CCC) Rightslink site.